

A material point time integration procedure for anisotropic, thermo rheologically simple, viscoelastic solids

H. Poon, M. F. Ahmad

236

Abstract This study presents an effective and robust time integration procedure for general anisotropic, thermal rheologically simple viscoelasticity, that is suitable for implementation in a broad spectrum of general purpose nonlinear finite element programs. It features a judicious choice of state variables which record the extent of inelastic flow (creep), a stable backward Euler integration step, and a consistent tangent operator. Numerical examples involving homogeneous stress states such as uniaxial tension and simple shear, and non-uniform stress states such as a beam under tip load, were carried out by incorporating the present scheme into a general purpose FEM package. Excellent agreement with analytical results is observed.

1

Introduction

Finite element simulations of viscoelastic behavior have been widely reported in the literature. The vast majority of them, however, deal with the isotropic case where there are only two distinct sets of relaxation behavior – one associated with the shear modulus and the other with bulk modulus. Examples of this line of work include Taylor et al. (1970), Henriksen (1984), Simo (1987), Lai and Bakker (1996), Kaliske and Rothert (1997), to name just a few. Additional literature review may be found in Yi (1991) and Zocher et al. (1997).

Certain materials of engineering interest exhibit anisotropic viscoelastic behavior. An example is thermosetting matrix composites during curing. Depending on the arrangement of fibers, the level of anisotropy is at least orthotropic, with 9 distinct modulus components, each with

its individual relaxation behavior. Up to 36 components can be expected in the truly anisotropic case.

Yi and Hilton (1995), Yi et al. (1996), and Yi et al. (1997) have carried out finite element simulations with anisotropic viscoelasticity, mostly dealing with curing induced residual stress calculations of thermoset composites. Their finite element algorithm is detailed in Yi and Hilton (1994) and Yi (1991). In brief, the approach starts from the constitutive relation, applies the viscoelastic version of the variational principle, invokes finite element discretization, and arrives at a system of integral equations in the nodal unknowns. By employing techniques such as the Laplace transform, it is possible to march forward in time by keeping the solutions from the previous two time steps, thus obtaining the transient time history without too much memory burden.

Zocher et al. (1997) presented a novel finite element scheme for linear anisotropic viscoelasticity. Rather than dealing with integral equations, the authors introduced a smart integration point constitutive update algorithm whereby the stress increment is separated into a part which is linear in the strain increment, and a nonlinear contribution which can be computed from stored results in the previous increment. Consequently, the overall incremental virtual work equation is linear in the displacement increment, bypassing the need for Newton iterations and the consistent tangent operator. However, the assumption of a single reduced time for all directions may be physically unrealistic for certain materials, such as fiber-reinforced composites.

This paper presents an alternate integration point constitutive update algorithm very similar in spirit to Zocher et al. (1997) mentioned above. Following Yi and Hilton (1995), the reduced time is directional dependent. An intelligent choice of state variables leads to evolution laws in the form of linear first order ODE's, the time integration of which can be achieved by a variety of common methods, e.g. backward Euler. Most importantly, the method is fully compatible with standard nonlinear finite element analysis, where the incremental virtual work equation is nonlinear in the displacement increment, requiring techniques such as Newton-Raphson iterations and consistent tangent operators.

2

Anisotropic viscoelastic model

It should be stated at the outset that the summation convention for repeated indices is inhibited in this work. All summations are explicitly indicated by summation signs.

Communicated by S. N. Atluri, 26 November 1997

H. Poon, M.F. Ahmad
National Center for Supercomputing Applications,
University of Illinois at Urbana-Champaign,
405 North Mathews Avenue, Urbana, IL 61801, USA

Correspondence to: F. Ahmad

The computational aspect of this work was performed at the National Center for Supercomputing Applications (NCSA) of the University of Illinois at Urbana-Champaign (UIUC). The authors wish to acknowledge the support of the NCSA staff and consultants.

2.1

Basic constitutive relations

Starting from the following hereditary integral relationship between stress and strain in a general anisotropic setting:

$$\sigma_{ij}(t) = \int_0^t \sum_k \sum_l C_{ijkl} (\zeta_{ijkl} - \zeta'_{ijkl}) \frac{d}{dt'} (\epsilon_{kl} - \epsilon_{kl}^*) dt' . \quad (1)$$

For anisotropy, the reduced time, which characterizes thermal rheologically simple behavior, can be different for different directions. Hence it can be written as

$$\zeta_{ijkl} = \int_0^t \frac{dt'}{A_{ijkl}(\theta(t'), \alpha(t'))} . \quad (2)$$

ζ'_{ijkl} has a similar definition, with integration up to t' . Here, the shift factor A is made dependent not only on temperature θ , but also on some other scalar variable α relevant to the application. For composites, moisture and degree of cure are two possible candidates for α .

The non-mechanical, stress-free strain is expressed as

$$\epsilon_{kl}^* = \int_{\theta_0}^{\theta} b_{kl}(s) ds + \int_{\alpha_0}^{\alpha} c_{kl}(s) ds \quad (3)$$

where b_{kl} are the thermal expansion coefficients. So the first term is thermal strain and c_{kl} are the α analogs.

In the interest of algebraic simplicity, the Prony series which characterizes modulus relaxation behavior takes the following form (considering only one exponential term):

$$C_{ijkl}(\zeta_{ijkl}) = C_{ijkl}^{\infty} + \tilde{C}_{ijkl} \exp\left(-\frac{\zeta_{ijkl}}{\tau_{ijkl}}\right) \quad (4)$$

where C_{ijkl}^{∞} are the equilibrium moduli, \tilde{C}_{ijkl} the magnitudes of transient decay, and τ_{ijkl} the relaxation times.

Multiple exponential terms can be handled with ease, as explained in a later subsection. To focus on the main ideas one exponential term is used in the foregoing development.

Substituting the Prony series (4) into (1) results in

$$\sigma_{ij}(t) = \int_0^t \sum_k \sum_l \left[C_{ijkl}^{\infty} + \tilde{C}_{ijkl} \exp\left(-\frac{\zeta_{ijkl} - \zeta'_{ijkl}}{\tau_{ijkl}}\right) \right] \times \frac{d}{dt'} (\epsilon_{kl} - \epsilon_{kl}^*) dt' . \quad (5)$$

Next the definition

$$C_{ijkl}^0 = C_{ijkl}^{\infty} + \tilde{C}_{ijkl} \quad (6)$$

can readily be interpreted as the instantaneous (glassy) moduli. Eq. (5) can be re-written as

$$\begin{aligned} \sigma_{ij}(t) &= \int_0^t \sum_k \sum_l \left\{ C_{ijkl}^0 - \tilde{C}_{ijkl} \right. \\ &\quad \times \left[1 - \exp\left(-\frac{\zeta_{ijkl} - \zeta'_{ijkl}}{\tau_{ijkl}}\right) \right] \left. \right\} \\ &\quad \times \frac{d}{dt'} \bar{\epsilon}_{kl} dt' \\ &= \sum_k \sum_l C_{ijkl}^0 (\epsilon_{kl} - \epsilon_{kl}^*) - \sigma_{ij}^c \end{aligned} \quad (7)$$

where σ_{ij}^c is a fictitious ‘‘creep’’ stress, being defined as the difference between the purely elastic stress based on instantaneous moduli and the actual stress. The following notation has been adopted for convenience:

$$\bar{\epsilon}_{kl} = \epsilon_{kl} - \epsilon_{kl}^* . \quad (8)$$

2.2

Choice of state variables

The proper choice of state variables is an important aspect in the design of the present viscoelastic time integration procedure. Ideally, those variables should follow clearly defined evolution laws and their values easily updated from one time increment to the next, preferably without knowledge of their entire time history. With this in mind, the following state variables were chosen:

$$D_{ijkl} = \int_0^t \tilde{C}_{ijkl} \left[1 - \exp\left(-\frac{\zeta_{ijkl} - \zeta'_{ijkl}}{\tau_{ijkl}}\right) \right] \dot{\bar{\epsilon}}_{kl} dt' \quad (9)$$

where $\dot{\phi} \equiv d\phi/dt'$, i.e. an over dot denotes differentiation w.r.t. the dummy time variable.

Note that D_{ijkl} exhibits minor symmetry: $D_{ijkl} = D_{jikl} = D_{ijlk}$, so that there are at most 36 distinct scalars to keep track of in the general anisotropic case. Also, the ‘‘creep’’ stress is merely the $k-l$ summation of these state variables:

$$\sigma_{ij}^c = \sum_k \sum_l D_{ijkl} . \quad (10)$$

2.3

A differentiation formula

In preparation for deriving the evolution law of D_{ijkl} , a formula for differentiating functions of the form

$$y(\tau) = \int_0^{\tau} f(\tau, \tau') d\tau' \quad (11)$$

with respect to τ , was developed.

Denoting by $\Delta\tau$ an infinitesimal change in τ , the following is observed:

$$\begin{aligned} y(\tau + \Delta\tau) - y(\tau) &= \int_0^{\tau + \Delta\tau} f(\tau + \Delta\tau, \tau') d\tau' - \int_0^{\tau} f(\tau, \tau') d\tau' \\ &= \int_{\tau}^{\tau + \Delta\tau} f(\tau + \Delta\tau, \tau') d\tau' \\ &\quad + \int_0^{\tau} [f(\tau + \Delta\tau, \tau') - f(\tau, \tau')] d\tau' \\ &\approx \int_{\tau}^{\tau + \Delta\tau} \left(f(\tau, \tau') + \frac{\partial f}{\partial x}(\tau, \tau') \Delta\tau \right) d\tau' \\ &\quad + \int_0^{\tau} \frac{\partial f}{\partial x}(\tau, \tau') \Delta\tau d\tau' \\ &\approx f(\tau, \tau) \Delta\tau + \frac{\partial f}{\partial x}(\tau, \tau) (\Delta\tau)^2 + \Delta\tau \int_0^{\tau} \frac{\partial f}{\partial x}(\tau, \tau') d\tau' \end{aligned} \quad (12)$$

where $\partial f/\partial x$ denotes the partial derivative of f w.r.t. its first argument. Following the definition of the derivative,

$$\begin{aligned} \frac{dy}{d\tau} &= \lim_{\Delta\tau \rightarrow 0} \frac{y(\tau + \Delta\tau) - y(\tau)}{\Delta\tau} \\ &= f(\tau, \tau) + \int_0^\tau \frac{\partial f}{\partial x}(\tau, \tau') d\tau'. \end{aligned} \quad (13)$$

2.4

Time evolution law for D_{ijkl}

The evolution law of D_{ijkl} can be derived as follows:

$$D_{ijkl} = \int_0^t \tilde{C}_{ijkl} \left[1 - \exp\left(-\frac{\zeta_{ijkl} - \zeta'_{ijkl}}{\tau_{ijkl}}\right) \right] \dot{\epsilon}_{kl} dt'. \quad (9)$$

Notice that ζ_{ijkl} is a function of t via Eq. (2). Similarly ζ'_{ijkl} is a function of t' . $\dot{\epsilon}_{kl} = d/dt' \bar{\epsilon}_{kl}$ is a function of t' . Therefore, the integrand is of the form $f(t, t')$ and the differentiation formula just developed can be applied. In this particular case,

$$f(t, t) = 0, \quad (14)$$

$$\frac{\partial f}{\partial x} = \tilde{C}_{ijkl} \exp\left(-\frac{\zeta_{ijkl} - \zeta'_{ijkl}}{\tau_{ijkl}}\right) \dot{\epsilon}_{kl} \frac{1}{\tau_{ijkl}} \frac{1}{A_{ijkl}} \quad (15)$$

where the last factor comes from the differentiation of (2) and A_{ijkl} is to be evaluated at time t . Finally, the time evolution law takes the form:

$$\begin{aligned} \frac{d}{dt} D_{ijkl} &= \int_0^t \tilde{C}_{ijkl} \exp\left(-\frac{\zeta_{ijkl} - \zeta'_{ijkl}}{\tau_{ijkl}}\right) \dot{\epsilon}_{kl} \frac{1}{\tau_{ijkl} A_{ijkl}} dt' \\ &= \frac{1}{\tau_{ijkl} A_{ijkl}} \int_0^t \tilde{C}_{ijkl} \exp\left(-\frac{\zeta_{ijkl} - \zeta'_{ijkl}}{\tau_{ijkl}}\right) \dot{\epsilon}_{kl} dt' \\ &= \frac{1}{\tau_{ijkl} A_{ijkl}} [\tilde{C}_{ijkl} \bar{\epsilon}_{kl} - D_{ijkl}]. \end{aligned} \quad (16)$$

2.5

Summary

The present constitutive law is summarized as follows:

$$\sigma_{ij}(t) = \sum_k \sum_l \left(C_{ijkl}^0 (\epsilon_{kl} - \epsilon_{kl}^*) - D_{ijkl} \right) \quad (17)$$

where

$$D_{ijkl} = \int_0^t \tilde{C}_{ijkl} \left[1 - \exp\left(-\frac{\zeta_{ijkl} - \zeta'_{ijkl}}{\tau_{ijkl}}\right) \right] \dot{\epsilon}_{kl} dt' \quad (9)$$

with its time evolution

$$\frac{d}{dt} D_{ijkl} = \frac{1}{\tau_{ijkl} A_{ijkl}} [\tilde{C}_{ijkl} \bar{\epsilon}_{kl} - D_{ijkl}]. \quad (16)$$

The achievement of such a differential (rate) form for the evolution of state variables is the high point in our algorithmic development. It offers the user great flexibility in choosing a suitable time integration method, such as

backward-Euler or trapezoidal rule, based on ease of coding and accuracy considerations. Perhaps more importantly, it obviates the need for non-physical assumptions such as linear time variation of strain throughout the increment. Such assumptions are adopted in many viscoelastic constitutive updating schemes such as the one in Zocher et al. (1997).

2.6

Generalization to multiple exponential terms

It suffices to illustrate the case for two exponential terms, where the relaxation modulus takes the form:

$$\begin{aligned} C_{ijkl}(\zeta_{ijkl}) &= C_{ijkl}^\infty + \tilde{C}_{ijkl} \exp\left(-\frac{\zeta_{ijkl}}{\tilde{\tau}_{ijkl}}\right) \\ &\quad + \tilde{C}_{ijkl}^* \exp\left(-\frac{\zeta_{ijkl}}{\tilde{\tau}_{ijkl}^*}\right). \end{aligned}$$

The hereditary constitutive relation is then:

$$\begin{aligned} \sigma_{ij}(t) &= \int_0^t \sum_k \sum_l \left[C_{ijkl}^\infty + \tilde{C}_{ijkl} \exp\left(-\frac{\zeta_{ijkl} - \zeta'_{ijkl}}{\tilde{\tau}_{ijkl}}\right) \right. \\ &\quad \left. + \tilde{C}_{ijkl}^* \exp\left(-\frac{\zeta_{ijkl} - \zeta'_{ijkl}}{\tilde{\tau}_{ijkl}^*}\right) \right] \\ &\quad \times \frac{d}{dt'} (\epsilon_{kl} - \epsilon_{kl}^*) dt'. \end{aligned}$$

The definition of the glassy moduli is revised as:

$$C_{ijkl}^0 = C_{ijkl}^\infty + \tilde{C}_{ijkl} + \tilde{C}_{ijkl}^*$$

resulting in the following rearranged equation:

$$\begin{aligned} \sigma_{ij}(t) &= \int_0^t \sum_k \sum_l \left\{ C_{ijkl}^0 \right. \\ &\quad \left. - \tilde{C}_{ijkl} \left[1 - \exp\left(-\frac{\zeta_{ijkl} - \zeta'_{ijkl}}{\tilde{\tau}_{ijkl}}\right) \right] \right. \\ &\quad \left. - \tilde{C}_{ijkl}^* \left[1 - \exp\left(-\frac{\zeta_{ijkl} - \zeta'_{ijkl}}{\tilde{\tau}_{ijkl}^*}\right) \right] \right\} \\ &\quad \frac{d}{dt'} (\epsilon_{kl} - \epsilon_{kl}^*) dt' \\ &= \sum_k \sum_l \{ C_{ijkl}^0 (\epsilon_{kl} - \epsilon_{kl}^*) - D_{ijkl} - E_{ijkl} \} \end{aligned}$$

where D_{ijkl}, E_{ijkl} are the chosen state variables, defined as:

$$\begin{aligned} D_{ijkl} &= \int_0^t \tilde{C}_{ijkl} \left[1 - \exp\left(-\frac{\zeta_{ijkl} - \zeta'_{ijkl}}{\tilde{\tau}_{ijkl}}\right) \right] \dot{\epsilon}_{kl} dt', \\ E_{ijkl} &= \int_0^t \tilde{C}_{ijkl}^* \left[1 - \exp\left(-\frac{\zeta_{ijkl} - \zeta'_{ijkl}}{\tilde{\tau}_{ijkl}^*}\right) \right] \dot{\epsilon}_{kl} dt'. \end{aligned}$$

Clearly, the evolution laws for D_{ijkl} and E_{ijkl} are completely analogous to that described in Sect. 2.4.

To summarize, addition of more exponential terms in the Prony series translates into more storage requirements and the added bookkeeping costs needed to update the extra state variables, but introduces no conceptual difficulty.

3 Computational aspects

In a typical ‘implicit’ finite element program which employs nonlinear material models, the discretized principle of virtual work, which enforces equilibrium and boundary conditions in a weak sense, generates an estimated incremental displacement field which is used to calculate integration point values of the stress and other field variables at the end of a time increment. If these stresses do not satisfy the principle of virtual work, then the estimate of the incremental displacement field is revised and new increment end stresses are calculated; iteration continues until the principle of virtual work is satisfied to within acceptable tolerances.

Within this context, the FEM program’s ‘constitutive update subroutine’, being called once for each integration point for each global iteration, must perform the following functions.

Input:

1. the (converged values of) stress, strain, state variables, etc. at time n
2. the (estimated) strain and perhaps other field variables¹ at time $n + 1$

Output:

1. the stress and state variables at time $n + 1$
2. the consistent tangent operator to be used in a Newton type iterative method

4 Implicit time integration

Focusing on the computational task at hand and adding superscripts to indicate the time step, the present constitutive law can be re-written as:

$$\sigma_{ij}^{n+1}(t) = \sum_k \sum_l \left(C_{ijkl}^0 \left(\epsilon_{kl}^{n+1} - \epsilon_{kl}^{*n+1} \right) - D_{ijkl}^{n+1} \right) . \quad (18)$$

Analyzing the right hand side terms, the following are noted:

1. ϵ_{kl}^{n+1} is a given, as mentioned in item 2 of input.

$$2. \epsilon_{kl}^{*n+1} = \int_{\theta_0}^{\theta^{n+1}} b_{kl}(s) ds + \int_{\alpha_0}^{\alpha^{n+1}} c_{kl}(s) ds . \quad (19)$$

As per item 2 of input, θ^{n+1} and α^{n+1} are given and ϵ_{kl}^{*n+1} is readily computed.

3. The only non-trivial task lies in computing D_{ijkl}^{n+1} . As mentioned in Sect. 2.5, the user is free to choose an appropriate method for integrating Eq. (16). The backward Euler scheme is implemented here for ease of

coding. Alternate strategies such as the generalized trapezoidal rule (“alpha” = 0.5), can be adopted without difficulty.

Replacing the derivative by finite difference in (16), and using the backward Euler scheme which is known for its stability, the following can be obtained:

$$\frac{D_{ijkl}^{n+1} - D_{ijkl}^n}{\Delta t} = \frac{1}{\tau_{ijkl} A_{ijkl}^{n+1}} \left[\tilde{C}_{ijkl} \bar{\epsilon}_{kl}^{n+1} - D_{ijkl}^{n+1} \right] . \quad (20)$$

Rearranging yields

$$D_{ijkl}^{n+1} = \left(\frac{1}{\Delta t} + \frac{1}{\tau_{ijkl} A_{ijkl}^{n+1}} \right)^{-1} \left[\frac{D_{ijkl}^n}{\Delta t} + \frac{\tilde{C}_{ijkl} \bar{\epsilon}_{kl}^{n+1}}{\tau_{ijkl} A_{ijkl}^{n+1}} \right] . \quad (21)$$

Again, A_{ijkl}^{n+1} is known since θ^{n+1} and α^{n+1} are also provided as per item 2 of input. Therefore D_{ijkl}^{n+1} is computable.

5 Consistent tangent operator (CTO)

The Consistent tangent operator concept was introduced by Simo and Taylor (1985) in the context of rate-independent plasticity. During the incremental solution process for nonlinear problems, nonlinear virtual work equations are solved by Newton’s method. In updating the global “Jacobian” matrix, estimates are needed, at the integration point level, of the rate of change of stress w.r.t. strain. Previously, the quantity $\partial \dot{\sigma} / \partial \dot{\epsilon}$ was used, resulting in sub-optimal convergence rates. It turns out that using the quantity $\partial \sigma^{n+1} / \partial \Delta \epsilon$ produces better results because this expression depends not only on the constitutive law but also on the time integration algorithm in the constitutive update. The use of this quantity, namely the consistent tangent operator, preserves the quadratic convergence rate of Newton’s method, accelerates the search for displacement fields that better satisfy the principle of virtual work.

The present simple constitutive update algorithm (18), (21) leads to a straightforward derivation of the CTO:

$$\begin{aligned} \frac{\partial D_{ijkl}^{n+1}}{\partial \Delta \epsilon_{ab}} &= \left(\frac{1}{\Delta t} + \frac{1}{\tau_{ijkl} A_{ijkl}^{n+1}} \right)^{-1} \frac{\tilde{C}_{ijkl}}{\tau_{ijkl} A_{ijkl}^{n+1}} \delta_{ka} \delta_{lb} , \\ \frac{\partial \sigma_{ij}^{n+1}}{\partial \Delta \epsilon_{ab}} &= \sum_k \sum_l \left(C_{ijkl}^0 \delta_{ka} \delta_{lb} - \left(\frac{1}{\Delta t} + \frac{1}{\tau_{ijkl} A_{ijkl}^{n+1}} \right)^{-1} \right. \\ &\quad \left. \times \frac{\tilde{C}_{ijkl}}{\tau_{ijkl} A_{ijkl}^{n+1}} \delta_{ka} \delta_{lb} \right) \quad (22) \\ &= C_{ijab}^0 - \left(\frac{1}{\Delta t} + \frac{1}{\tau_{ijab} A_{ijab}^{n+1}} \right)^{-1} \frac{\tilde{C}_{ijab}}{\tau_{ijab} A_{ijab}^{n+1}} \\ &= C_{ijab}^0 - \frac{\Delta t}{\Delta t + \tau_{ijab} A_{ijab}^{n+1}} \tilde{C}_{ijab} . \end{aligned}$$

The temperature dependence of the reduced time expression in Eq. (2) signals that heat transfer may also be an integral part of the FEM analysis. In such case, the Consistent tangent operator w.r.t. temperature is also needed. The following derivation is provided for completeness.

¹ e.g. temperature, if heat transfer is involved

$$\begin{aligned}
\frac{\partial \epsilon_{kl}^{*n+1}}{\partial \Delta \theta} &= \frac{\partial}{\partial \Delta \theta} \int_{\theta_0}^{\theta^{n+1}} b_{kl}(s) ds = b_{kl}(\theta^{n+1}), \\
\frac{\partial D_{ijkl}^{n+1}}{\partial \Delta \theta} &= \left(\frac{1}{\Delta t} + \frac{1}{\tau_{ijkl} A_{ijkl}^{n+1}} \right)^{-1} \frac{-\tilde{C}_{ijkl}}{\tau_{ijkl} A_{ijkl}^{n+1}} b_{kl}(\theta^{n+1}) \\
&= -\frac{\Delta t}{\Delta t + \tau_{ijkl} A_{ijkl}^{n+1}} \tilde{C}_{ijkl} b_{kl}(\theta^{n+1}), \\
\frac{\partial \sigma_{ij}^{n+1}}{\partial \Delta \theta} &= \sum_k \sum_l \left(-C_{ijkl}^0 b_{kl}(\theta^{n+1}) \right. \\
&\quad \left. + \frac{\Delta t \tilde{C}_{ijkl}}{\Delta t + \tau_{ijkl} A_{ijkl}^{n+1}} b_{kl}(\theta^{n+1}) \right) \\
&= -\sum_k \sum_l \left(C_{ijkl}^0 - \frac{\Delta t \tilde{C}_{ijkl}}{\Delta t + \tau_{ijkl} A_{ijkl}^{n+1}} \right) \\
&\quad \times b_{kl}(\theta^{n+1}).
\end{aligned} \tag{23}$$

6

Numerical examples

To illustrate how the current algorithm can be implemented in a general purpose FEM code, a ‘user material’ subroutine UMAT, which serves precisely the function of the constitutive update discussed in Sect. 3, was developed. The FEM code ABAQUS was chosen and linked with this subroutine.

Examples 1 and 2 primarily serve to validate the anisotropic capability of the user subroutine, using very simple loading conditions of uniaxial tension and simple shear. Example 3 tests the time integration procedure in a more general setting with stress gradients, namely a cantilever beam subjected to a tip load.

For Examples 1 and 2, the hypothetical viscoelastic material was chosen to be orthotropic, with principal directions along the 1,2,3 axes. The precise material properties are shown in Table 1. Material characterizations for Example 3 will be described later.

Note that ν_{ij} is the Poisson’s ratio that characterizes the transverse strain in the j -direction, when the material is stressed in the i -direction. In general, ν_{ij} is not equal to ν_{ji} ; they are related by $\nu_{ij}/E_i = \nu_{ji}/E_j$.

These values completely determine the glassy relaxation moduli C_{ijkl}^0 and the equilibrium relaxation moduli C_{ijkl}^∞ .

Table 1. Glassy and equilibrium moduli

moduli	glassy value	equilibrium value
E_1	2.8	0.23
E_2	2.7	0.22
E_3	2.6	0.21
ν_{21}	0.3	0.3
ν_{31}	0.3	0.3
ν_{32}	0.3	0.3
G_{12}	1	0.08
G_{13}	0.9	0.075
G_{23}	0.8	0.07

The transient decay \tilde{C}_{ijkl} is given by

$$\tilde{C}_{ijkl} = C_{ijkl}^0 - C_{ijkl}^\infty.$$

The time period of simulation was chosen as $0 \leq t \leq 1$. Also, the relaxation times were set to

$$\tau_{2222} = 0.09,$$

$$\tau_{3333} = 0.08,$$

$$\tau_{1313} = \tau_{1331} = \tau_{3113} = \tau_{3131} = 0.09,$$

$$\tau_{2323} = \tau_{2332} = \tau_{3223} = \tau_{3232} = 0.08, \text{ and}$$

$$\tau_{ijkl} = 0.1 \text{ for the rest.}$$

In the interest of obtaining manageable analytical solutions, reduced time shifting as indicated in Eq. (2) and non-mechanical strain as shown in Eq. (3) were not considered. The anisotropic model tested takes the simpler form:

$$\sigma_{ij}(t) = \int_0^t \sum_k \sum_l C_{ijkl}(t-t') \frac{d}{dt'} \epsilon_{kl} dt'$$

with

$$C_{ijkl}(t) = C_{ijkl}^\infty + \tilde{C}_{ijkl} \exp\left(-\frac{t}{\tau_{ijkl}}\right).$$

Example 1. Uniaxial tension

Here, the material sample is subjected to an applied stress $\sigma(t)$ in the 1-direction, and free of stress in other directions. The non-zero strain components are $\epsilon_{11}, \epsilon_{22}, \epsilon_{33}$. Denoting by B_{ijkl} the creep compliance analog of C_{ijkl} , the analytical solution becomes

$$\begin{aligned}
\epsilon_{11}(t) &= \int_0^t B_{1111}(t-\tau) \frac{d\sigma}{d\tau}(\tau) d\tau, \\
\epsilon_{22}(t) &= \int_0^t B_{2211}(t-\tau) \frac{d\sigma}{d\tau}(\tau) d\tau, \\
\epsilon_{33}(t) &= \int_0^t B_{3311}(t-\tau) \frac{d\sigma}{d\tau}(\tau) d\tau.
\end{aligned} \tag{24}$$

The linear stress history is prescribed as:

$$\sigma(t) = \frac{t}{1000}, \quad 0 \leq t \leq 1.$$

The ultimate stress is of the order 10^{-3} of Young’s modulus, conforming to the small strain theory.

Calculating the creep compliance $B_{ijkl}(t)$ from the prescribed relaxation moduli $C_{ijkl}(t)$ represents the key computational effort. This involves taking and inverting Laplace transforms. More precisely, let matrix $[C(t)]$ represent the condensed form of $C_{ijkl}(t)$, and similarly for $[B(t)]$. Then, the elementwise Laplace transform of $[B(t)]$, denoted by $[\bar{B}(s)]$ will equal to

$$[\bar{B}(s)] = \frac{1}{s^2} [\bar{C}(s)]^{-1}.$$

The software package Mathematica is used to perform such a conversion, as well as the final integration of Eq. (24) to obtain the analytical solution.

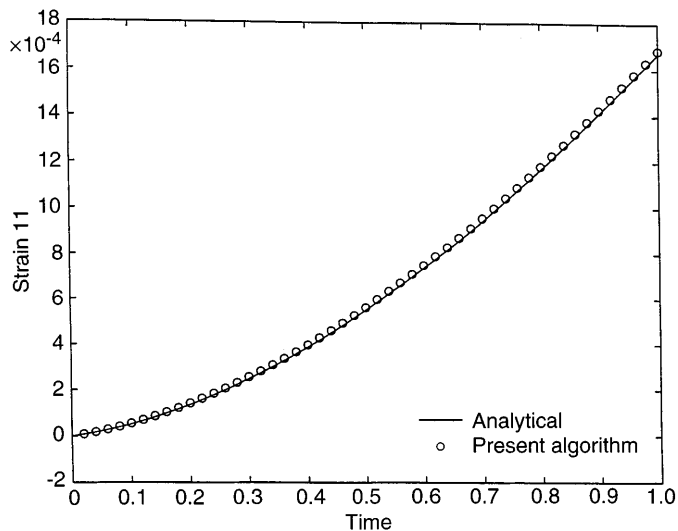


Fig. 1. Uniaxial tension: strain 11

The present time integration scheme was validated by performing a finite element analysis of a 3D problem with 50 equal increments.

Example 2. Simple shear

Here, the material sample is subjected to an applied shear strain

$$\epsilon_{12}(t) = \frac{t}{1000} .$$

The analytical solution becomes

$$\begin{aligned} \sigma_{12}(t) &= \int_0^t C_{1212}(t-\tau) \frac{d\epsilon_{12}}{d\tau} + C_{1221}(t-\tau) \frac{d\epsilon_{21}}{d\tau} d\tau \\ &= 2 \int_0^t C_{1212}(t-\tau) \frac{d\epsilon_{12}}{d\tau} d\tau . \end{aligned}$$

The situation is even simpler in this case since the creep compliance $B_{ijkl}(t)$ is not needed. Again, a 3-D FEM analysis incorporating the present time integra-

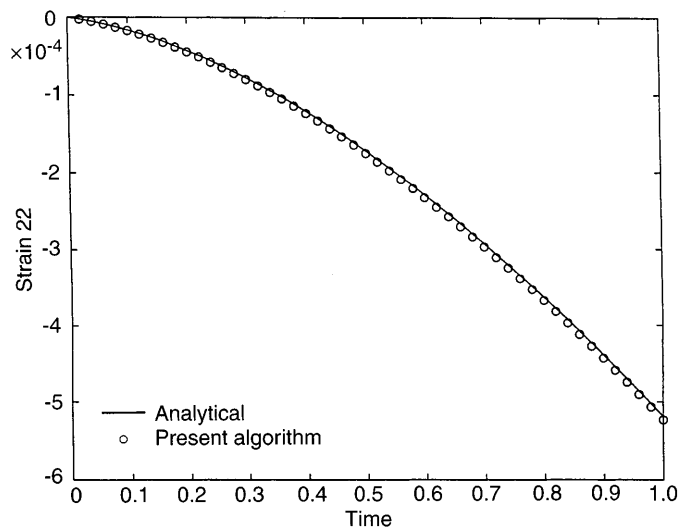


Fig. 2. Uniaxial tension: strain 22

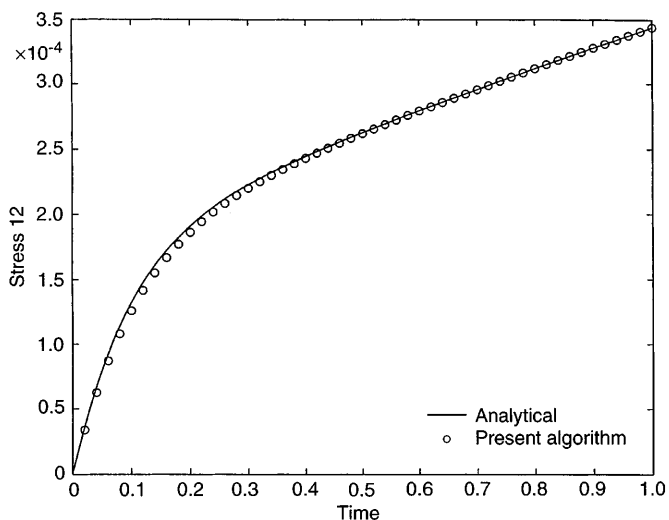


Fig. 4. Simple shear: stress 12

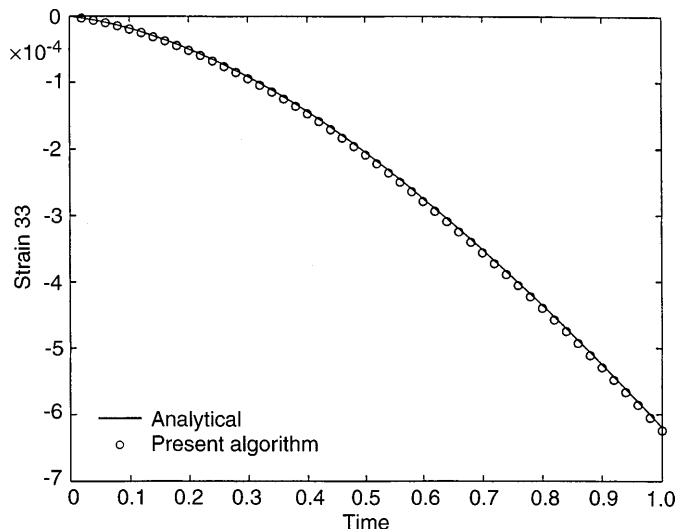


Fig. 3. Uniaxial tension: strain 33

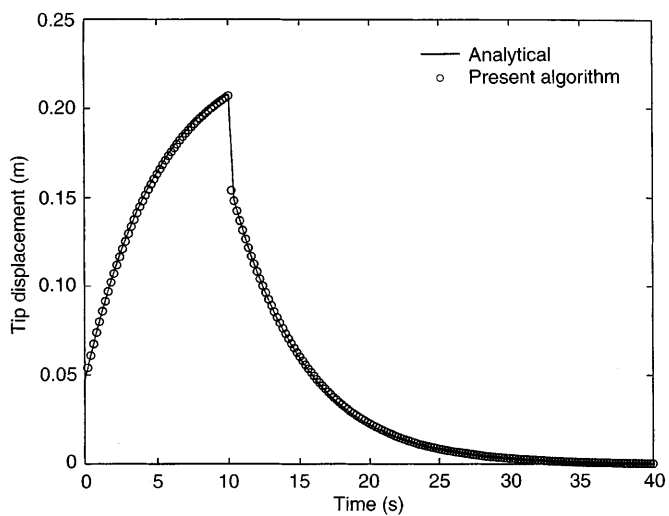


Fig. 5. Beam with tip load: tip displacement

tion procedure was performed with 50 equal increments.

Example 3. Beam with tip load

This example serves to verify the present viscoelastic time integration method in a more complex setting with spatially varying stress states. A cantilever beam is subjected to a transient concentrated tip load

$$P = P_0[H(t) - H(t - t_1)]$$

where $P_0 = 1$ N, $t_1 = 10$ s, and H is the Heavyside function. The beam has a length, L , of 18 m and a square cross section of area $A = 1$ m².

According to classical Euler-Bernoulli beam theory, the tip displacement w_L in the linearly elastic case is given by:

$$w_L = \frac{P_0 L^3}{3EI}$$

where I is the area moment of inertia of the cross section (in this case $\frac{1}{12}$ m⁴). The hypothetical viscoelastic material has the following relaxation behavior for the Young's modulus:

$$E(t) = E_\infty + E_1 \exp(-t/\rho) \quad (25)$$

The values of E_∞ , E_1 and ρ are taken to be 0.1 MPa, 0.4 MPa and 1 second respectively.

Applying the standard viscoelastic correspondence principle yields the tip displacement time history:

$$w_L = \frac{P_0 L^3}{3I} [D(t) - D(t - t_1)H(t - t_1)]$$

where the creep compliance $D(t)$ is given by:

$$D(t) = D_0 + D_1(1 - \exp(-t/\lambda))$$

with

$$E_0 \equiv E_\infty + E_1, \quad D_0 \equiv \frac{1}{E_0}, \quad D_1 \equiv \frac{1}{E_\infty} - \frac{1}{E_0}, \quad \lambda \equiv \frac{E_0 \rho}{E_\infty}.$$

It should be noted that the beam theory solution approaches the 3-D elasticity solution for slender beams such as the present one whose aspect ratio is 18.

By virtue of the 1-D nature of classical beam theory, only the Young's modulus in the axial direction enters into the picture. Transverse Young's moduli and Poisson ratios do not matter as far as beam theory is concerned. For simplicity the hypothetical material is chosen to be isotropic with Young's modulus described in (25), and a constant Poisson's ratio of 0.3.

The 3-D finite element analysis employed a uniform mesh of $20 \times 2 \times 2$ elements, with a constant time step of 0.2 second.

7

Conclusion

This study demonstrates the supreme accuracy and effectiveness of a novel time integration procedure for anisotropic, small strain, thermal rheologically simple viscoelasticity. The scheme performs constitutive updates at the integration point level. Its unconventional choice of state variables allows for stress updating without reference to information from previous increments. While the stable backward Euler strategy accommodates bigger time steps, the Consistent tangent operator minimizes the number of global iterations. Its elegant structure renders it generalizable to multiple Prony exponential terms. Most importantly, its non-interference with the global finite element framework means it can be readily incorporated into general purpose nonlinear structural analysis codes. Validation of the present scheme has been performed in various settings involving both homogeneous and non-uniform stress states.

References

- Henriksen M (1984) Non-linear viscoelastic stress analysis - a finite element approach. *Comp and Struct*. 18:133-139
- Kaliske M, Rothert H (1997) Formulation and implementation of three-dimensional viscoelasticity at small and finite strains. *Comput. Mech*. 19:228-239
- Lai J, Bakker A (1996) 3-D schapery representation for non-linear viscoelasticity and finite element implementation. *Comput. Mech*. 18:182-191
- Simo JC (1987) On a fully three-dimensional finite strain viscoelastic damage model: formulation and computational aspects. *Comput. Meth. Appl. Mech. Eng*. 60:153-173
- Simo JC, Taylor RL (1985) Consistent tangent operators for rate-independent elastoplasticity. *Comput. Meth. Appl. Mech. Eng*. 48:101-118
- Taylor RL, Pister KS, Goudreau GL (1970) Thermomechanical analysis of viscoelastic solids. *Int. J. Num. Meth. Eng*. 2:45-59
- Yi S (1991) Finite element analysis of anisotropic viscoelastic composite structures and analytical determination of optimum viscoelastic material properties. Ph.D. Thesis, University of Illinois at Urbana-Champaign, USA
- Yi S, Hilton H (1994) Dynamic finite element analysis of viscoelastic composite plates in the time domain. *Int. J. Num. Meth. Eng*. 37:4081-4096
- Yi S, Hilton H (1995) Hygrothermal effects on viscoelastic responses of laminated composites. *Composites Eng*. 5:183-193
- Yi S, Hilton H, Ahmad MF (1996) Nonlinear thermo-viscoelastic analysis of interlaminar stresses in laminated composites. *J. Appl. Mech*. 63:218-224
- Yi S, Ahmad MF, Hilton H (1997) Finite element algorithms for dynamic simulations of viscoelastic composite shell structures using conjugate gradient method on coarse grained and massively parallel machines. *Int. J. Num. Meth. Eng*. 40:1857-1875
- Zocher MA, Groves SE, Allen DH (1997) A three-dimensional finite element formulation for thermoviscoelastic orthotropic media. *Int. J. Num. Meth. Eng*. 40:2267-2288